Viscoelasticity of randomly branched polymers in the critical percolation class

Charles P. Lusignan
Department of Physics and Astronomy, University of Rochester, Rochester, New York 14627

Thomas H. Mourey
Analytical Technology Division, Eastman Kodak Company, Rochester, New York 14650-2136

John C. Wilson
Office Imaging, Eastman Kodak Company, Rochester, New York, 14650-2129

Ralph H. Colby*
Imaging Research and Advanced Development, Eastman Kodak Company, Rochester, New York, 14650-2109
(Received 15 May 1995)

We report viscosity, recoverable compliance, and molecular weight distribution of a series of randomly branched polyester samples below their gel point. From the static characterization we determine $\tau = 2.17 \pm 0.08$ (95%) for the exponent controlling the mass distribution, indicating that this system belongs to the critical percolation universality class. We find that viscosity diverges at the gel point with an exponent $s = 1.36 \pm 0.09$ (95%), in agreement with a simple bead-spring (Rouse) model without hydrodynamic or topological interactions. Similarly, the recoverable compliance diverges at the threshold with an exponent $t = 2.71 \pm 0.30$ (95%), consistent with the idea that $k_B T$ of elastic energy is stored per correlation volume. The complex shear modulus obeys a power law in frequency with exponent $u = 0.659 \pm 0.015$ (95%), thereby confirming the dynamical scaling law $u = t/(s+t)$.

PACS number(s): 61.41.+e, 82.70.Gg

INTRODUCTION

Percolation theory models the evolution of molecular structure during random branching processes. Two static universality classes are known. The mean-field class, modeled by Flory-Stockmayer theory [1–3], describes vulcanization [4,5], the cross-linking of long polymer chains. Critical percolation describes the polymerization of small multifunctional monomers [6–8], or longer chains cross-linked in solution [9–11]. An arbitrary experimental system may exhibit a crossover between mean-field behavior far from the gel point and critical behavior close to the transition. The static structure class observed depends on the experimental measurement range, the degree of polymerization N between cross-links [12,13], and the solvent concentration [14].

In contrast to the molecular structure, the rheology of randomly branched polymers is not well understood. Cursory inspection of the literature indicates apparent nonuniversal dynamics, and hence a plethora of contradicting theories have been proposed. We contend that real progress in this field can only be made by *simultaneously characterizing both the molecular structure and the rheology of near critical branched polymers*. In this work, molten polyester samples with $N \cong 2$ are prepared by polycondensation under conditions of unbalanced

---

*Present address: Department of Materials Science and Engineering, The Pennsylvania State University, University Park, PA 16802.

stoichiometry. We are thus able to prepare the stable samples necessary to determine the molecular weight distribution and measure the viscosity and recoverable compliance near the gel point. From analysis of the structural and rheological data we conclude that a simple bead-spring model [15–18], without hydrodynamic or topological interactions, models the rheology of randomly branched molecules in the critical percolation class.

BACKGROUND THEORY

As in continuous thermodynamic phase transitions [19], scaling forms are now well established for the various quantities of interest near the percolation threshold, and it is convenient to parametrize them in terms of the relative extent of reaction

$$\varepsilon = \frac{|p - p_c|}{p_c} , \tag{1}$$

where p is the number of cross-links formed and p_c is the number required to reach the gel point. Below we review the static scaling relationships [8] necessary for our discussion, and summarize the percolation and vulcanization class exponent values in Table I.

STATIC STRUCTURE

The number fraction of branched polymers with mass M is a power law in M that is truncated at high molecular weight by an exponential cutoff function f,

$$n(M) \sim M^{-\tau} f(M/M_{\text{char}}) , \tag{2}$$

TABLE I. Static exponents for percolation. Error bounds are 95% confidence intervals from pooling the results of all calculations (in three dimensions) listed in [21]. The pooling was done using weighted averages [22] with 95% confidence intervals as weights.

	τ	γ	σ	ν
Critical percolation	2.20 ± 0.05	1.78 ± 0.09	0.452 ± 0.011	0.879 ± 0.020
Vulcanization	$5/2$	1	$1/2$	$1/2$

where the exponent τ controls the system's polydispersity. The characteristic largest molecular mass M_{char} diverges as the gel point is approached,

$$M_{char} \sim \varepsilon^{-1/\sigma} . \tag{3}$$

A number of measurable quantities are ratios of the moments of the molecular weight distribution through

$$M_q = \frac{\int n(M)M^q dM}{\int n(M)M^{q-1}dM} . \tag{4}$$

The ratio with $q=2$ yields the weight-average molecular mass M_w, which diverges at the critical point as

$$M_w \sim \varepsilon^{-\gamma} . \tag{5}$$

Higher order moment ratios, such as $q=3$ for the z-average molecular mass M_z, are all proportional to the characteristic largest molecular weight M_{char} [8]. The radius of gyration of the branched polymer with mass M_{char} is the characteristic size (correlation length) ξ for gelation. It diverges at the threshold as

$$\xi \sim \varepsilon^{-\nu} . \tag{6}$$

Experimental determination of ε requires measuring the extent of reaction p and the critical extent of reaction p_c. Unfortunately, the relative uncertainty in ε diverges at the gel point [20]. We circumvent this problem by correlating two measured quantities that can be measured with reasonable precision. We determine the exponent τ from

$$M_{char} \sim (M_w)^{1/\sigma\gamma} \sim (M_w)^{1/(3-\tau)} , \tag{7}$$

using the scaling law [8]

$$3 - \tau = \sigma\gamma \tag{8}$$

to cast the exponent solely in terms of τ. Equations (2)–(8) apply for both critical percolation and vulcanization, with different sets of exponent values in each class (see Table I). The exponent ν is related to the other static exponents in critical percolation through hyperscaling [8,23],

$$3\nu = \frac{(\tau-1)}{\sigma} . \tag{9}$$

In the mean-field limit the Fisher law [19] plays a corresponding role:

$$\nu = \frac{\gamma}{2} = \frac{(3-\tau)}{2\sigma} . \tag{10}$$

Consequently both classes have only two independent static exponents.

DYNAMIC RESPONSE

The shear stress relaxation modulus $G(t)$ and the complex shear modulus $G^*(\omega)$ obey power laws in time and frequency in the vicinity of the gel point [24–26]:

$$G(t) \sim t^{-u}, \quad G^*(\omega) \sim (i\omega)^u . \tag{11}$$

The zero shear rate viscosity η and the steady state recoverable compliance J_e^0 are related to $G(t)$ for linear response [27], and below the critical point they diverge with exponents s and t:

$$\eta = \int_0^\infty G(t)dt \sim \varepsilon^{-s} , \tag{12}$$

$$J_e^0 = \frac{1}{\eta^2} \int_0^\infty tG(t)dt \sim \varepsilon^{-t} . \tag{13}$$

Beyond the gel point, the recoverable compliance and the equilibrium shear modulus G_e are reciprocally related [27], so the same exponent t also describes the growth of modulus above the gel point

$$G_e \cong \frac{1}{J_e^0} \sim \varepsilon^t . \tag{14}$$

The three dynamic exponents are interrelated through the dynamical scaling law [25,26]

$$u = \frac{t}{(s+t)} , \tag{15}$$

so that there are only two independent dynamic exponents. The numerical values for these exponents depend on the model chosen for the dynamic response. We defer consideration of potential models until the discussion section below.

We utilize ε-independent relationships to evaluate exponent ratios for the dynamic quantities just as we did for the static ones in (7):

$$\eta \sim (M_w)^{s/\gamma} \sim (M_{char})^{s\sigma} \tag{16}$$

for viscosity and

$$J_e^0 \sim (M_w)^{t/\gamma} \sim (M_{char})^{t\sigma} \tag{17}$$

for recoverable compliance. Viscosity and recoverable compliance are correlated through

$$J_e^0 \sim \eta^{t/s} \sim \eta^{u/(1-u)} . \tag{18}$$

EXPERIMENT

Polyester synthesis

Hydroxy terminated polyesters with very low acid number were prepared from adipic acid (AD) and

trimethylolpropane (TMP). Feed ratios were determined with the aid of the POLYESTER RESIN CALCULATIONS program available from Eastman Chemical Company. Entering arguments were for a polyester with acid number zero, a polymer yield of 250 g, and a variable number of molecular weights.

Appropriate amounts of AD and TMP were weighed into a triple neck 500 ml round bottom flask along with 0.25 g of Fascat 4100 (butyl stannoic acid). The flask was fitted with a Teflon blade stirrer, Teflon bearing, nitrogen inlet, and a steam heated partial condensing packed column with a water cooled distillation head. The flask was them immersed in a 200 °C salt bath and continuously stirred from 1.75 to 3.75 h collecting the water distillate formed. The bath temperature was then increased to 220 °C and stirring was continued for 24–31 h. At this stage, the branched polymer was stirred under water aspirator vacuum for approximately 0.5 h and then poured from the flask into amber storage jars and cooled to room temperature. Samples were stored under dry nitrogen to minimize the absorption of water. All samples had acid numbers of 0.017 meq/g or less as determined by non-aqueous titration. This demonstrates the complete reaction of all the acid groups.

Size exclusion chromatography

The multidetector size exclusion chromotography (SEC) apparatus and accompanying techniques are similar to those described previously [20,28,29]. A PD2000W two-angle light scattering (TALLS) detector (Precision Detectors, Inc.) was installed in the thermostated chamber of a Waters model 410 differential refractive index (DRI) detector and connected in series before the DRI cell. Light scattering intensities were measured simultaneously at 15° and 90°. Details of the data analysis for this instrument are provided elsewhere [30,31].

The eluent was uninhibited tetrahydrofuran (THF). All samples were prefiltered through 0.2 μm Anatop inorganic membranes and injected in 100 μl amounts. No filters were inserted between the columns and the detectors. In THF the AD-TMP polyester has a specific refractive index increment $dn/dc = 0.0710$ ml/g. The effective interdetector volume between the TALLS and DRI detectors was determined using the systematic approach described in [32]. This method also provides some correction for axial dispersion in multidetector SEC [33].

Three 7.5 mm diam $\times$ 300 mm Polymer Labs 5 μm particle diameter mixed-C PLgel columns were used (at a nominal flow rate of 1.0 ml/min) for samples with $M_w < 5 \times 10^4$. Sample concentrations ranged from 2.0 (highest molecular weights) to 6.0 mg/ml (lowest molecular weights). Samples with $M_w > 5 \times 10^4$ were analyzed with four 7.5 mm diam $\times$ 300 mm^2 Polymer Labs mixed-A PLgel columns. These columns have nominal particle sizes of 20 μm and are designed specifically for high molecular weight materials. A flow rate of 0.6 ml/min with sample concentrations between 0.2 and 2.0 mg/ml minimized shear degradation.

We report M_w obtained from integration of the 15° light scattering signal, without the DRI. This integration method is unaffected by axial dispersion and error in interdetector volume determination. It has been shown to provide the most accurate and precise measure of M_w by SEC with light scattering detection [28,30,31]. M_{max} is taken as the average elution volume corresponding to peak output signals from both the 15° and 90° light scattering detectors [10,11,34]. In principal, M_w and M_z can also be calculated from the light scattering and DRI detector signals. However, these methods rely on extrapolation techniques in the low signal regions of both detectors; consequently the tails of the distribution have a significant amount of uncertainty. We view these quantities as auxiliary measurements to be compared with M_w (from light scattering only) and M_{max}. We find excellent agreement between the two M_w values, and also that $M_z/M_{max} = 0.99 \pm 0.22$ (95%) as expected from previous studies [10,11,20,34]. From (2) and its moment ratios (4) one expects $M_{max} \propto M_z \propto M_{char}$. Typical average molecular weight uncertainties are on the order of $\pm 10\%$ for M_w, $\pm 12\%$ for M_{max}, and $\pm 20\%$ for M_z. All data reported in Table II are averages of between six and eight replicate SEC analyses. Figure 1 is a plot of M_{max} against M_w on logarithmic scales, with slope $1/(\sigma\gamma) = 1.20 \pm 0.11$ (95%). Using (8) we obtain

$$\tau = 2.17 \pm 0.08 \ (95\%) \ .$$

A similar analysis for M_z versus M_w gave $\tau = 2.20 \pm 0.12$ (95%) in agreement with the more precise M_{max} versus M_w determination.

The number density of polymers with mass M was calculated from the DRI and TALLS data as in [35] and then fitted to a power law times a shifted Gaussian cutoff
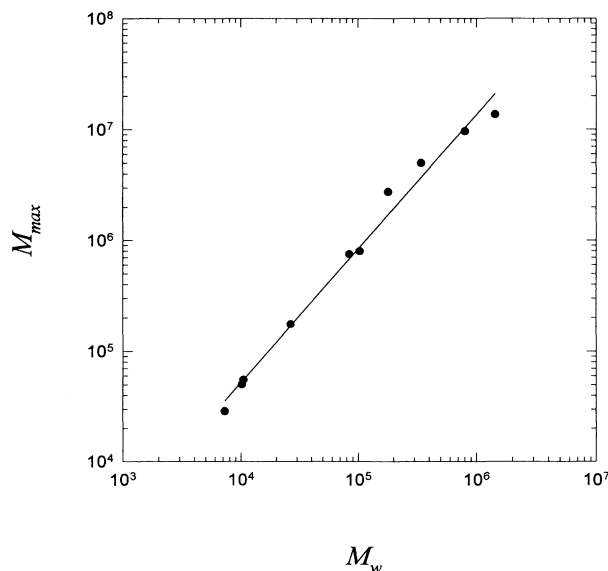

FIG. 1. Correlation of the characteristic largest molecular weight M_{max} with the weight-average molecular weight M_w.

TABLE II. Experimental data.

M_w	M_{max}	M_z	M_{char}	T_g (°C)	η (P)[a]	η (P)[b]	J_e^0 (cm^2/dyn)
7.31×10^3	2.89×10^4	2.06×10^4	1.34×10^4	-37	1.51×10^3	2.19×10^3	2.32×10^{-6}
1.02×10^4	5.03×10^4	4.37×10^4	2.51×10^4	-34	2.53×10^3	2.53×10^3	4.80×10^{-6}
1.05×10^4	5.52×10^4	4.76×10^4	2.65×10^4	-34	2.62×10^3	2.62×10^3	4.52×10^{-6}
2.66×10^4	1.75×10^5	1.94×10^5	7.48×10^4	-33	4.87×10^3	4.32×10^3	1.11×10^{-5}
8.38×10^4	7.50×10^5	8.26×10^5	6.30×10^5	-33	1.48×10^4	1.31×10^4	6.73×10^{-5}
1.03×10^5	7.98×10^5	1.36×10^6	6.64×10^5	-33	1.64×10^4	1.45×10^4	9.18×10^{-5}
1.80×10^5	2.74×10^6	2.49×10^6	1.57×10^6	-35	1.86×10^4	2.10×10^4	1.53×10^{-4}
3.44×10^5	5.00×10^6	3.79×10^6	2.94×10^6	-36	2.73×10^4	3.49×10^4	3.44×10^{-4}
8.04×10^5	9.63×10^6	9.30×10^6	5.57×10^6	-32	8.45×10^4	6.66×10^4	4.44×10^{-3}
1.44×10^6	1.37×10^7	1.72×10^7	1.14×10^7	-33	1.36×10^5	1.21×10^5	1.07×10^{-2}

[a]Viscosity data taken at 30 °C.
[b]Viscosity data adjusted to $T_g + 64$ K using the WLF equation (21).

function [11,36] of the form

$$n(M) = A \left[\frac{M}{M_{char}} \right]^{-\tau}$$

$$\times \exp \left\{ - \left[z_{max} - \left[\frac{M}{M_{char}} \right]^{\sigma} \right]^2 \right\}, \quad (19)$$

assuming the percolation values of τ and σ (see Table I). The constant $z_{max} = 0.681$ was calculated according to the procedure in [36,37] and depends only on τ, σ, and the functional form of (19). A two-parameter fit determined the prefactor A and M_{char} for each sample, the latter being listed in Table II. Figure 2 is representative of the quality of the fit of (19) to the SEC data for the sample farthest from the gel point. Plotting M_{char} versus M_{max} yields

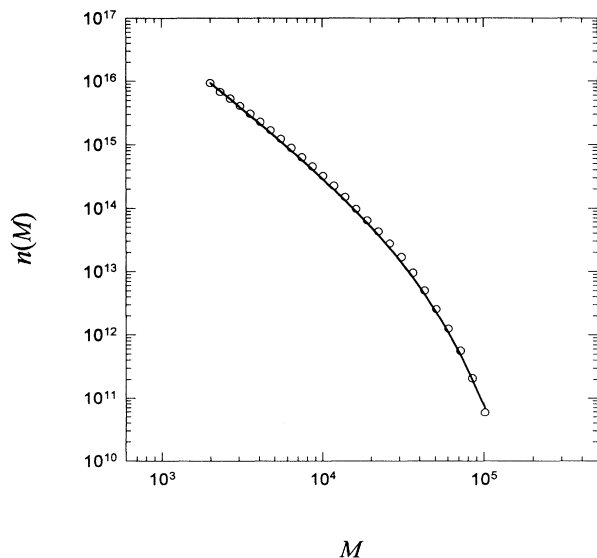$$M_{char}/M_{max} = 0.59 \pm 0.12 \ (95\%) \ .$$

FIG. 2. SEC data (every 20th point) for the sample with $M_w = 7310$. The curve is a two-parameter nonlinear fit to (19) using the percolation values for the exponents τ and σ from Table I and $z_{max} = 0.681$ calculated as in [36].

Oscillatory shear

Oscillatory strain experiments were conducted in a Rheometrics System Four mechanical spectrometer using 25 mm diameter parallel plates. Samples were heated (never exceeding 80 °C) until they could be conveniently poured onto the plate fixtures insuring minimal stress during transfer. Characterization was performed under a nitrogen atmosphere to prevent the absorption of water. Sample heights near 1 mm were used for all samples, and frequencies from 0.1 to 100 rad/s were probed at each of the four test temperatures 0, 15, 30, and 60 °C. Strain sweeps at 100, 10, 1 and 0.1 rad/s were used to determine the range of strain amplitudes corresponding to linear viscoelastic response. Only strains corresponding to linear response were used during the frequency sweeps. SEC performed on samples taken from the rheometer indicates that no measurable sample degradation occurred during loading or testing [38,39].

Time-temperature superposition [27] was used to collapse the data at different temperatures onto master curves according to the empirical formula

$$G^*(\omega; T) = b_T G^*(a_T \omega; T_0) \ , \quad (20)$$

where a_T and b_T are material constants and $T_0 = 30$ °C, a reference temperature. The modulus scale shifts b_T were found to be of order unity and the frequency scale shifts followed the WLF equation [27]

$$\log_{10}(a_T) = \frac{-C_1(T - T_g)}{(C_2 + T - T_g)} \ . \quad (21)$$

The glass transition temperatures T_g were taken as the midpoint of a 10 K/min heating scan in a Perkin-Elmer DSC 7 differential scanning calorimeter, and are listed in Table II. The WLF constants C_1 and C_2 were independent of the degree of cross-linking with values $C_1 = 6.33 \pm 0.48$ (95%) and $C_2 = 120 \pm 10$ K (95%) near the "typical" values for linear polymers [27] of $C_1 = 8.86$ and $C_2 = 101.2$ K. Our finding that the temperature dependence of the viscoelastic response is independent of extent of reaction ε is consistent with recent work on randomly end-linked polycaprolactone [40]. Our results conclusively show that the *viscosity exponent s and modulus exponent t are temperature independent*. Previ-
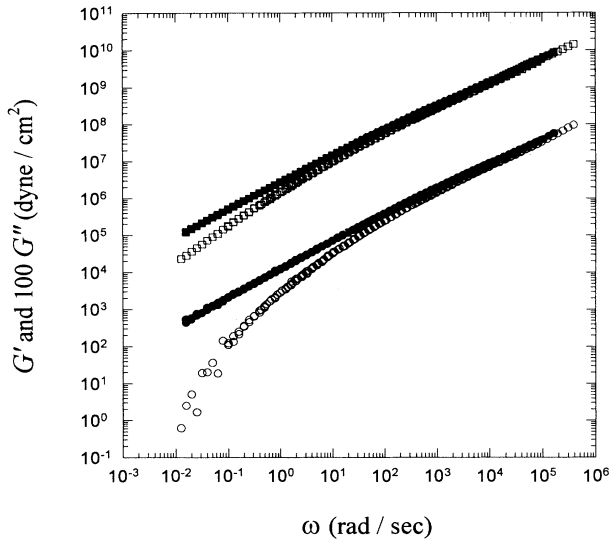
FIG. 3. Master curves for the storage modulus G' (circles) and loss modulus G'' (squares) for two representative samples: $M_w = 1.80 \times 10^5$ (open symbols), $M_w = 1.44 \times 10^6$ (filled symbols). The loss modulus values G'' have been multiplied by 100 for clarity.

ous work with polyurethane [41] indicated that s was temperature dependent. The principal difference between the polyurethane and the polyester is that the former exhibits a pronounced change in glass transition temperature with extent of reaction ε [42], whereas the data in Table II show that the polyester system's T_g remains relatively insensitive to extent of reaction. These results suggest that systems known to be in the critical percolation class should have a universal dynamic response provided that T_g changes are minimal in the critical region.

Representative master curves for the sample closest to the gel point and one much further away are shown in Fig. 3. Note that at high frequencies the master curves for both G' and G'' overlap and obey a power law in frequency whose slope fixes the value for the stress relaxation exponent u. Averaging the values obtained from both curves results in

$$u = 0.650 \pm 0.020 \ (95\%) \ .$$

Creep and recovery

Creep and subsequent recovery were performed using a computerized version of Plazek's frictionless magnetic bearing torsional creep rheometer [43]. This instrument is ideal for measuring the terminal response for near critical systems where the longest relaxation time diverges at the gel point. Creep times of approximately 10^6 s were necessary to achieve steady state for the samples closest to the gel point, and multiple determinations were made. Characterization was performed in parallel plate geometry under nitrogen atmosphere at a constant temperature of 30.0 ± 0.1 °C.

Near the gelation threshold the apparent viscosity depends strongly on shear rate [38,39]. Experimental shear

rates were varied by at least a factor of 5 to ensure that they corresponded to the linear (zero shear rate) limit. Samples close to the gel point required shear rates of 5×10^{-5} s^{-1}, and SEC analysis confirmed that the samples remained stable throughout the several weeks the experiments lasted. By using samples below the gel point, and probing with sufficiently low shear rates, the sample degradation problems for near critical gels reported by Venkataraman and Winter [38,39] were avoided.

Once steady state is reached in the creep experiment, the strain (angular deflection) varies linearly with time and the viscosity η is the ratio of the applied stress to the measured shear rate (the time rate of change of the strain) [27]. Viscosity data, taken at 30 °C, are listed in Table II along with viscosity values, at $T_g + 64$ K, calculated using (21). The latter are plotted against M_w and M_{max} in Fig. 4. Using (16) we determine

$$s/\gamma = 0.760 \pm 0.038 \ (95\%) \ ,$$

$$s\sigma = 0.620 \pm 0.076 \ (95\%) \ .$$

After evaluating the viscosity in steady state creep, the applied stress is removed and the angular elastic recoil (recoverable strain) is monitored as a function of time. The total recovered strain is divided by the applied stress used during creep to calculate the recoverable compliance J_e^0 [27]. The recoverable compliance was found to be temperature independent between 0 and 30 °C for polyester samples whose viscosity was greater than 10^4 P at 30 °C. For samples with viscosity below 10^4 P at 30 °C we measured recoverable compliance at 0 °C to eliminate inertial effects that interfere with the recoverable strain measurement (note that $\eta > 10^5$ P for all the samples at 0 °C). Recoverable compliance data are tabulated in Table II and plotted against M_w and M_{max} in Fig. 5, from which we use (17) to conclude

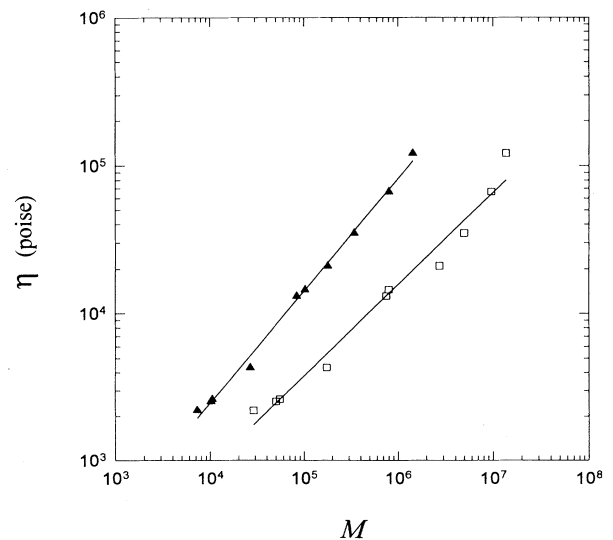$$t/\gamma = 1.52 \pm 0.18 \ (95\%), \quad t\sigma = 1.23 \pm 0.25 \ (95\%) \ .$$

FIG. 4. Viscosity η as functions of weight-average molecular weight M_w (filled symbols) and characteristic largest molecular weight M_{max} (open symbols).
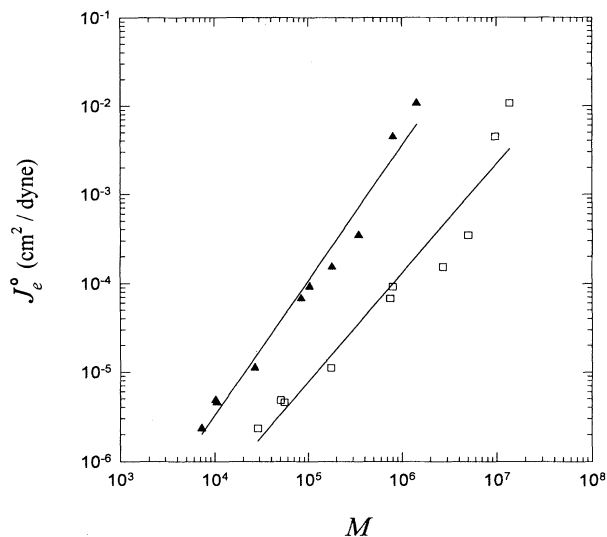
FIG. 5. Recoverable compliance J_e^0 as functions of weight-average molecular weight M_w (filled symbols) and characteristic largest molecular weight M_{max} (open symbols).

In Fig. 6, recoverable compliance is plotted against viscosity with a slope $t/s = u/(1-u) = 1.96 \pm 0.18$ (95%), providing an additional measurement of

$$u = 0.667 \pm 0.022 \ (95\%) \ ,$$

in agreement with the value 0.650 ± 0.020 (95%) obtained from the oscillatory strain measurements.

DISCUSSION

Critical percolation correctly models the molecular structure for systems with small degrees of polymerization N between cross-links [6,23,44–46]. Our experimentally determined value of $\tau = 2.17 \pm 0.08$ places this po-
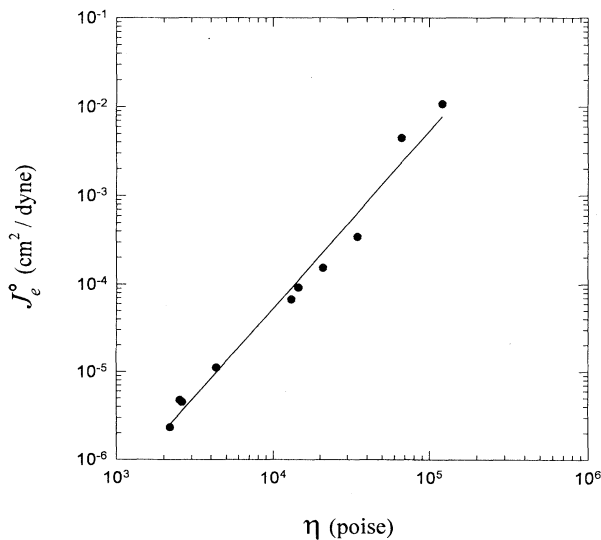

FIG. 6. Correlation of recoverable compliance J_e^0 with viscosity η.

TABLE III. Experimental exponent determinations. Error bounds are 95% confidence intervals.

Exponent	Source	Value
τ	Figure 1 and (7)	2.17 ± 0.08
s	s/γ in Fig. 4[a]	1.35 ± 0.10
s	$s\sigma$ in Fig. 4[a]	1.37 ± 0.17
s	pooled estimate[b]	1.36 ± 0.09
s	calculated via (27)[c]	1.36 ± 0.06
t	t/γ in Fig. 5[a]	2.71 ± 0.35
t	$t\sigma$ in Fig. 5[a]	2.72 ± 0.56
t	pooled estimate[b]	2.71 ± 0.30
t	calculated via (25)[c]	2.60 ± 0.15
u	G' and G'' in Fig. 3	0.650 ± 0.020
u	t/s in Fig. 6 and (18)	0.667 ± 0.022
u	pooled estimate[b]	0.659 ± 0.015
u	calculated via (28)[c]	0.657 ± 0.058

[a]Percolation values (Table I) for γ and σ were used to extract exponent from measured ratio. Error bounds were determined by propagation of errors [22] and 95% confidence intervals were calculated from the standard deviation of the linear regression slope [47].
[b]Pooling accomplished by weighted average [22] using 95% confidence intervals as weights.
[c]Measured τ and theoretical critical percolation σ used in Rouse expressions to calculate the dynamic exponent.

lyester system (with $N = 2$) in the critical percolation universality class. Further confirmation comes from Fig. 2, where the mass distribution was successfully fitted to (19) using $\tau = 2.20$ and $\sigma = 0.452$. Consequently, we utilize the known static exponents for critical percolation (see Table I) to extract the dynamic exponents s and t from the measured exponent ratios. Table III catalogs our experimental determinations of exponents τ, s, t, and u.

The literature abounds with different predictions for the dynamic exponents s and t. We summarize the main results for s in Table IV and t in Table V. Since the only theory to correctly predict our observed dynamic exponents is the branched polymer Rouse model, we briefly review its essential physics below and refer the reader to the literature for further details; see [15–18] and references therein.

Rouse model

The original Rouse model mapped linear polymer molecules onto a system of identical beads and springs [27,57] and has been extended to branched polymer molecules [15–18]. The model asssumes no hydrodynamic interaction between beads through the surrounding medium; an approximation that should be valid in molten polymer systems (no solvent) where hydrodynamic interactions are believed to be screened beyond the monomer size scale [7]. The Rouse model is known to describe the rheology of short (unentangled) linear polymer melts [27,57].

For critical percolation, molecules of a given mass can only overlap significantly with smaller polymers [58].

TABLE IV. Viscosity exponent predictions. Error bounds are 95% confidence intervals.

	s	s/γ	$s\sigma$	Reference
Rouse model	1.33±0.02	0.747±0.046	0.601±0.019	[15–18,48]
Superconductivity analogy	0.665±0.010	0.374±0.023	0.301±0.010	[49,50]
Experiment	1.36±0.09[a]	0.760±0.038	0.620±0.076	this work

[a]Pooled estimate from Table III.

This suggests that interchain interactions, such as entanglements, may not be important for dynamics in this limit. If each molecule relaxes stress independently, the self-similar molecular mass distribution [Eq. (2)] implies the existence of a self-similar relaxation time distribution [59]. This spectrum is the essence of the dynamic scaling hypothesis and from it one calculates the entire viscoelastic response.

In the Rouse model each bead contributes equally to the friction coefficient ζ of a given molecule. Thus ζ is proportional to the number of beads and the molecular mass. The largest branched polymer in the system, with mass M_{char} and size ξ, has a diffusion coefficient given by the Einstein relation

$$D \cong \frac{k_B T}{\zeta} \sim \frac{1}{M_{\text{char}}} . \tag{22}$$

The relaxation time $\mathcal{T}$ of the largest polymer (and hence the terminal relaxation time of the sample) is proportional to the time it takes this molecule to diffuse a distance roughly equal to its size

$$\mathcal{T} \cong \frac{\xi^2}{D} \sim M_{\text{char}}\xi^2 . \tag{23}$$

The stress relaxation modulus at time $\mathcal{T}$ is $k_B T$ per chain in the Rouse model. It is proportional to the reciprocal of the recoverable compliance. Since hyperscaling requires chains of size ξ to be at their overlap concentration [58], their number density is ξ^{-3} and

$$J_e^0 \cong \frac{\xi^3}{k_B T} . \tag{24}$$

Inserting (6), (9), and (13) into (24) leads to the modulus exponent

$$t = 3\nu = \frac{(\tau - 1)}{\sigma} , \tag{25}$$

which describes the divergence of J_e^0 below the gel point, and the growth of the elastic modulus G_e above it [18,51,60,61].

The viscosity is the product of the relaxation time and the modulus at that time,

$$\eta \sim \frac{\mathcal{T}}{J_e^0} \sim \frac{M_{\text{char}}}{\xi} . \tag{26}$$

Substituting (3), (6), and (12) into (26) gives the viscosity exponent

$$s = \frac{1}{\sigma} - \nu = \frac{(4 - \tau)}{3\sigma} . \tag{27}$$

Combining the dynamic scaling law (15) with (25) and (27) we find

$$u = \frac{t}{(s + t)} = \frac{3(\tau - 1)}{(1 + 2\tau)} , \tag{28}$$

so that u depends solely on τ. The calculated values of s, t, and u obtained by using the measured τ and critical percolation σ in (25), (27), and (28) agree very well with the experimental values of these exponents (see Table III).

Dynamic universality

A number of experimental studies have measured weight-average molecular mass and viscosity, thereby determining the ratio s/γ from (16). Bidstrup and Macosko [62], Gordon, Ward, and Whitney [63], and Colby, Gillmor, and Rubinstein [18] polymerized monomers and found $s/\gamma \approx 1$. Systems with short chains between branch points (small N) have s/γ near 1.0 in reasonable agreement with the Rouse prediction of 0.75 and clearly distinct from the superconductivity analogy prediction of 0.37. The fact that the reported $s/\gamma \approx 1$ values are slightly above the Rouse prediction may indicate that these systems lie in the crossover between the

TABLE V. Modulus exponent predictions. Error bounds are 95% confidence intervals.

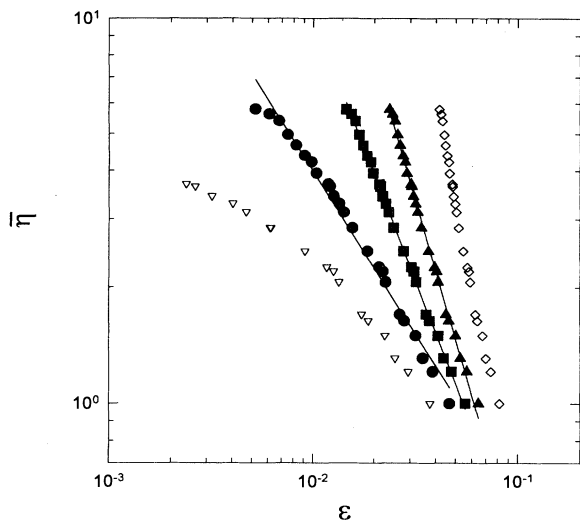|	t	t/γ	$t\sigma$	Reference
Rouse model	2.64±0.06	1.48±0.12	1.19±0.06	[16–18,51]
Conductivity analogy	1.99±0.09	1.12±0.11	0.899±0.064	[49,50,52]
Conductivity II	3.75±0.13	2.11±0.19	1.70±0.04	[53,54]
Rigidity I	4.4	2.5	2.0	[55]
Rigidity II	2.1	1.2	1.0	[56]
Rigidity III	3.8	2.2	1.7	[56]
Experiment	2.71±0.30[a]	1.52±0.18	1.23±0.25	this work

[a]Pooled estimate from Table III.

FIG. 7. Correlations of normalized viscosity $\bar{\eta}$ from Ref. [75] and relative reaction extent ε, assuming values for the gel time of 2080 min (open triangles), 2100 min (filled circles), 2120 min (filled squares), 2140 min (filled triangles), and 2180 min (open diamonds).

critical percolation and vulcanization limits. Only one group [18,20,34] determined that their system (with $N \approx 20$) indeed was in the crossover with an apparent $\tau = 2.35 \pm 0.03$ (95%).

Systems with longer chains between branch points have systematically higher apparent values for s/γ. End-linked polydimethylsiloxane (PDMS) [64] with $N \approx 50$ exhibits higher values of $s/\gamma = 1.5$ and $s/\gamma = 2.6$. Data on cross-linked polyethylenes [65,66], with 100 to 200 monomers between branch points, apparently have even larger values, with $3.3 \leq s/\gamma \leq 5.3$. We expect that entanglements will be important for long chain branching (large N) and may invalidate the dynamic scaling hypothesis in general and the Rouse model in particular. Entanglements are expected to make the viscosity a stronger function of molecular weight, and thus the apparent increase of s/γ with increasing N is not surprising.

Many measurements of the exponent u close to the gel point have been reported. Systems cross-linked in the melt (without solvent) follow a clear trend. The stress relaxation exponent decreases from $u \approx 0.7$ [25,46,67–69] for systems in the critical percolation class where $N \approx 1$ to $u \approx 0.5$ [24,70] as N increases. For very long chains between cross-links, Scanlan and Winter [71] observed even lower values near $u \approx 0.2$. Antonietti et al. [72] found that u decreased from 0.5 to 0.2 as N increased from 20 to 140. These findings are consistent with recent theoretical predictions that entanglement effects will lower the apparent u observed at high frequencies [73], with a crossover to the Rouse value of $u = 0.67$ only at very low frequencies when N is large.

Much experimental inquiry has focused on cross-linking in solution, but static and dynamic quantities have not been simultaneously determined for any of these

systems. Potential complications due to the competition between phase separation and gelation [7] as well as hydrodynamic interactions may have profound effects on the rheological properties, even if the static ones are modeled by critical percolation [6,10,11]. Consequently, we choose not to consider these systems here, focusing instead on solvent-free melts. Recognizing that the apparent dynamic exponents change for melt cross-linking when $N \gg 1$, we further restrict our discussion to the question of whether or not there are universal dynamic exponents for the critical percolation universality class with $N \approx 1$ in the melt.

In addition to the present work, three groups have measured both τ and u for the molten polymerization of monomers. Adam and co-workers [25,74] found $\tau = 2.20 \pm 0.04$ and $u = 0.72 \pm 0.02$. Trappe, Richtering, and Burchard [46] reported $\tau = 2.17 \pm 0.03$ and $u = 0.71 \pm 0.01$. Adolf, Martin, and Wilcoxon [67,68] measured $\gamma = 1.7 \pm 0.1$ (indicating critical percolation, see Table I) and $u = 0.70 \pm 0.05$. These results are all consistent with our findings, and are in agreement with the Rouse model predictions.

The only work reporting static exponents consistent with critical percolation and a dynamic exponent inconsistent with the Rouse predictions is [75]. For the same polyurethane system [74,75] $\tau = 2.20$, $u = 0.72$, $s \approx 0.8$, and $t \approx 3.2$. With the exception of s, these exponents are consistent with the Rouse model. Assuming (15) we calculate an expected value of $s = 1.37$ from t and u. The determination of s was made from data covering only a sixfold range in viscosity [75]. We are thus motivated to reexamine the viscosity data of [75]. The gel point was determined by linearizing a plot of $\log(\eta)$ versus $\log(\varepsilon)$ using a multiple parameter fitting procedure where the unknown prefactor, the gel point p_c, and exponent are strongly coupled. Small uncertainties in the gel point translate into large errors in the fitted exponent, as shown for the data of [75] in Fig. 7. Viscosity was measured as the polymerization reaction proceeded with reaction time assumed to be proportional to the extent of reaction ε. Using a gel time of 2100 min the authors concluded $s = 0.8 \pm 0.1$. Data for viscosity as a function of ε are presented in Fig. 7 for five choices of the gel time: 2080, 2100, 2120, 2140, and 2180 min. Gel times between 2100 and 2140 min (filled symbols) give reasonable conformance with (12). The smallest variance about the regression line corresponds to a gel time of approximately 2120 min and results in $s = 1.36$. Variations of $\pm 1\%$ around this gel time (filled symbols) drastically change the fitted value of s. Choosing a gel time of 2100 min yields $s = 0.8$, while a gel time of 2140 min gives $s = 1.8$. Without an independent measure of the critical point (which is unavailable for these data), the determination of critical exponents from data covering such a limited range is extremely imprecise and subjective. Gordon and Torkington discuss this and related issues in great detail [76].

Figure 7 illustrates not only the importance of measuring a wide range of viscosities, but also the crucial role molecular weight determinations play in evaluating critical exponents for gelation. Without static characterizations, or an *independent* knowledge of the gel point and a

wide experimental range, linearized extrapolation methods are incapable of measuring critical exponents with sufficient precision. In light of Fig. 7 we conclude that the data in [75] cannot be used to invalidate the Rouse model. Furthermore, we expect that the Rouse dynamics is indeed the universal viscoelastic response of randomly branched polymers in the critical percolation class.

CONCLUSION

We have measured the molecular mass distribution and the linear viscoelastic response of a series of near critical branched polyesters with roughly $N=2$ monomers between junction points. As expected, this system exhibits percolation class static structure, demonstrated by $\tau=2.17\pm0.08$. Molecular characterization has the advantage that it enables the determination of critical exponent ratios without relying on measurement of the gel point. Oscillatory shear measurements at different temperatures have determined the stress relaxation exponent $u=0.659\pm0.015$ and clearly show that dynamic critical exponents are temperature independent. By using a nearly frictionless torsional creep and recovery technique we determined the viscosity exponent $s=1.36\pm0.09$ and the modulus exponent $t=2.71\pm0.30$ below the gel point.

The measured u, s, and t confirm the dynamic scaling law $u=t/(s+t)$ and are in excellent agreement with the Rouse dynamic scaling model. While proof of universal dynamic exponents for critical percolation must await fu-

ture studies, we believe that such universality does exist for melt polymerized branched monomers ($N\approx1$). It is crucial that future studies measure both the molecular weight distribution and the viscoelastic properties of the same samples. Such simultaneous determinations allow evaluation of exponent ratios without requiring knowledge of the precise location of the gel point, making this a far superior method of extracting critical exponent values from experimental data than the traditional linearized extrapolation approach.

It is clear from inspection of the literature that the Rouse model does not hold for the rheology of branched polymers with long chain sections between branch points. We believe that these large N systems have their dynamics controlled by topological interactions between chains (entanglements). Such systems will be the subject of a future presentation.

ACKNOWLEDGMENTS

[1] P. J. Flory, J. Am. Chem. Soc. **63**, 3083 (1941).

[2] W. H. Stockmayer, J. Chem. Phys. **11**, 45 (1943).

[3] W. H. Stockmayer, J. Chem. Phys. **12**, 125 (1944).

[4] W. Burchard, Adv. Polym. Sci. **48**, 1 (1983).

[5] M. Gordon and S. B. Ross-Murphy, Pure Appl. Chem. **43**, 1 (1975).

[6] D. Stauffer, A. Coniglio, and M. Adam, Adv. Polym. Sci. **44**, 103 (1983).

[7] P. G. de Gennes, *Scaling Concepts in Polymer Physics* (Cornell University Press, Ithaca, 1988).

[8] D. Stauffer and A. Aharony, *Introduction to Percolation Theory*, 2nd ed. (Taylor and Francis, London, 1992).

[9] K. Kajiwara, W. Burchard, M. Kowalski, D. Nerger, K. Dusek, L. Matejka, and Z. Tuzar, Makromol. Chem. **185**, 2543 (1984).

[10] L. Leibler and F. Schosseler, Phys. Rev. Lett. **55**, 1110 (1985).

[11] F. Schosseler, H. Benoit, Z. Grubisic-Gallot, C. Strazielle, and L. Leibler, Macromolecules **22**, 400 (1989).

[12] P. G. de Gennes, J. Phys. (Paris) **38**, L355 (1977).

[13] S. Alexander, in *Physics of Finely Divided Matter,* edited by N. Boccara and M. Daoud (Springer-Verlag, New York, 1985).

[14] M. Daoud, J. Phys. (Paris) **37**, L201 (1979).

[15] P. G. de Gennes, C. R. Acad. Sci. Ser. B **286**, 131 (1978).

[16] M. Rubinstein, R. H. Colby, and J. R. Gillmor, in *Space-Time Organization in Macromolecular Fluids,* edited by F. Tanaka, M. Doi, and T. Ohta (Springer-Verlag, Heidelberg, 1989).

[17] J. E. Martin, D. A. Adolf, and J. P. Wilcoxon, Phys. Rev. A **39**, 1325 (1989).

[18] R. H. Colby, J. R. Gillmor, and M. Rubinstein, Phys. Rev. E **48**, 3712 (1993).

[19] K. Huang, *Statistical Mechanics,* 2nd ed. (Wiley, New York, 1987).

[20] R. H. Colby, M. Rubinstein, J. R. Gillmor, and T. H. Mourey, Macromolecules **25**, 7180 (1992).

[21] The mean-field (vulcanization) exponents are exact and well known in the literature; see [6,8]. Values for three-dimensional percolation represent a pooling of the series and Monte Carlo data summarized by J. Adler, Y. Meir, A. Aharony, and A. B. Harris, Phys. Rev. B **41**, 9183 (1990).

[22] J. R. Taylor, *An Introduction to Error Analysis: The Study of Uncertainties in Physical Measurements* (University Science Books, Mill Valley, 1982).

[23] M. Adam, D. Lairez, F. Boué , J. P. Busnel, D. Durand, and T. Nicolai, Phys. Rev. Lett. **67**, 3456 (1991).

[24] F. Chambon and H. H. Winter, Polym. Bull. **13**, 499 (1985).

[25] D. Durand, M. Delsanti, M. Adam, and J. M. Luck, Europhys. Lett. **3**, 297 (1987).

[26] H. H. Winter, Prog. Colloid Polym. Sci. **75**, 104 (1987).

[27] J. D. Ferry, *Viscoelastic Properties of Polymers,* 3rd ed. (Wiley, New York, 1980).

[28] T. H. Mourey, S. M. Miller, and S. T. Balke, J. Liq. Chromatogr. **13**, 435 (1990).

[29] T. H. Mourey, S. M. Miller, J. A. Wesson, T. E. Long,

and L. W. Kelts, Macromolecules **25**, 45 (1990).

[30] T. H. Mourey and H. Coll, in *Hyphenated Techniques in Polymer Characterization,* edited by T. Provder, Advances in Chemistry Vol. 247 (American Chemical Society, Washington, D.C., 1995), p. 123.

[31] T. H. Mourey and H. Coll, J. Appl. Polym. Sci. **56**, 65 (1995).

[32] T. H. Mourey and S. T. Balke, in *Chromatography of Polymers: Characterization by SEC and FFF,* edited by T. Provder, ACS Symposium Series Vol. 521 (American Chemical Society, Washington, DC, 1993).

[33] P. Cheung, R. Lew, S. T. Balke, and T. H. Mourey, J. Appl. Polym. Sci. **47**, 1701 (1993).

[34] E. V. Patton, J. A. Wesson, M. Rubinstein, J. C. Wilson, and L. E. Oppenheimer, Macromolecules **22**, 1946 (1989).

[35] T. Lew, D. Suwanda, and S. T. Balke, J. Appl. Polym. Sci. **35**, 1049 (1988).

[36] H. Ottavi, J. Phys. A **20**, 1015 (1987).

[37] C. P. Lusignan, Ph.D. dissertation, University of Rochester, 1995.

[38] S. K. Venkataraman and H. H. Winter, Rheol. Acta **29**, 423 (1990).

[39] S. K. Venkataraman, Ph.D. dissertation, University of Massachusetts, 1990.

[40] A. I. Izuka, H. H. Winter, and T. Hashimoto, Macromolecules **27**, 6883 (1994).

[41] D. Lairez, M. Adam, E. Raspaud, J. R. Emery, and D. Durand, Prog. Coll. Polym. Sci. **90**, 37 (1992).

[42] D. Durand (private communication).

[43] D. Plazek, J. Polym. Sci. A **6**, 621 (1968).

[44] J. Bauer and W. Burchard, J. Phys. (France) II **2**, 1053 (1992).

[45] J. Bauer and W. Burchard, Macromolecules **26**, 3103 (1993).

[46] V. Trappe, V. Richtering, and W. Burchard, J. Phys. (France) II **2**, 1453 (1992).

[47] R. L. Anderson, *Practical Statistics for Analytical Chemists* (Von Nostrand Reinhold, New York, 1987).

[48] S. Arbabi and M. Sahimi, Phys. Rev. Lett. **65**, 725 (1990).

[49] P. G. de Gennes, J. Phys. (Paris) **37**, L1 (1976).

[50] F. Devreux, J. P. Boilot, F. Chaput, L. Malier, and M. A. V. Axelos, Phys. Rev. E **47**, 2689 (1993).

[51] M. Daoud and A. Coniglio, J. Phys. A **14**, L301 (1981).

[52] M. Daoud, J. Phys. A **21**, L237 (1988).

[53] M. Sahimi, J. Phys. C **19**, L79 (1986).

[54] S. Roux, J. Phys. A **19**, L351 (1986).

[55] S. Feng and P. N. Sen, Phys. Rev. Lett. **52**, 216 (1984).

[56] S. Arbabi and M. Sahimi, Phys. Rev. B **47**, 703 (1993).

[57] M. Doi and S. F. Edwards, *The Theory of Polymer Dynamics* (Clarendon, Oxford, 1986).

[58] M. E. Cates, J. Phys. (Paris) Lett. **46**, L837 (1985).

[59] M. Daoud, J. Phys. A **21**, L973 (1988).

[60] J. E. Martin, D. Adolf, and J. P. Wilcoxon, Phys. Rev. Lett. **61**, 2620 (1988).

[61] M. Rubinstein and R. H. Colby, Macromolecules **27**, 3184 (1994).

[62] S. A. Bidstrup and C. W. Macosko, J. Polym. Sci. Polym. Phys. **28**, 691 (1990).

[63] M. Gordon, T. C. Ward, and R. S. Whitney, in *Polymer Networks,* edited by A. J. Chompff and S. Newman (Plenum, New York, 1971).

[64] E. M. Valles and C. W. Macosko, Macromolecules **12**, 521 (1979).

[65] A. Ram, Polym. Eng. Sci. **17**, 793 (1977).

[66] R. A. Mendelson, W. A. Bowels, and F. L. Finger, J. Polym. Sci. A2 **8**, 105 (1970).

[67] D. Adolf, J. E. Martin, and J. P. Wilcoxon, Macromolecules **23**, 527 (1990).

[68] D. Adolf and J. E. Martin, Macromolecules **23**, 3700 (1990).

[69] M. Takahashi, K. Yokoyama, T. Masuda, and T. Takigawa, J. Chem. Phys. **101**, 798 (1994).

[70] F. Chambon and H. H. Winter, J. Rheol. **30**, 367 (1986).

[71] J. C. Scanlan and H. H. Winter, Macromolecules **24**, 47 (1991).

[72] M. Antonietti, K. J. Fölsch, H. Sillescu, and T. Pakula, Macromolecules **22**, 2812 (1989).

[73] M. Rubinstein, S. Zurek, T. C. B. McLeish, and R. C. Ball, J. Phys. (Paris) **51**, 757 (1990).

[74] M. Adam, M. Delsanti, J. P. Munch, and D. Durand, Physica A **163**, 85 (1990).

[75] M. Adam, M. Delsanti, and D. Durand, Macromolecules **18**, 2285 (1985).

[76] M. Gordon and J. Torkington, Pure Appl. Chem. **53**, 1461 (1981).